Vibrational Spectroscopy and ab Initio Studies of Lithium Bis(oxalato)borate (LiBOB) in Different Solvents

Roman Holomb,[†,§] Wu Xu,[‡,⊥] Henrik Markusson,[†] Patrik Johansson,[*,†] and Per Jacobsson[†]

Department of Applied Physics, Chalmers University of Technology, Göteborg, SE−412 96, Sweden, and Department of Chemistry and Biochemistry, Arizona State University, Tempe, Arizona 85287-1604

Received: May 2, 2006; In Final Form: August 15, 2006

The effect of lithium ion coordination with the bis(oxalato)borate (BOB^-) $[B(C_2O_4)_2]^-$ anion in DMSO, PEG, PPG, and d-PPG has been studied in detail by IR and Raman spectroscopy. Ab initio calculations were performed to allow a consistent analysis of the experimental data. The main features observed in the IR and Raman spectra correspond to the presence of "free", un-coordinated, BOB^- anions. Only with use of d-PPG as solvent a small amount of $Li^+\cdots BOB^-$ ion pairs were detected. The Raman spectra and the calculations together indicate that Li^+ coordinates bidentately with two end-oxygen atoms of the BOB^- anion. The identification of ion pairs can be used to reveal limitations of LiBOB based electrolytes. The results for LiBOB are compared with literature on other Li salts.

1. Introduction

Energy storage electronic devices and improvement of their functional properties is very important at present. Rechargeable batteries are one of the most often used important portable power sources for electronic devices (mobile phones, digital cameras, laptops, etc.). Considerable attention now is concentrated on lithium rechargeable batteries as these batteries provide paramount higher energy densities than other concepts. Still, the improvement of several practically significant properties of these devices, such as capacity, lifetime and their cost, urges for research and development. The Li ion containing electrolyte, whether liquid, polymer, or gel, is perhaps the one component of the batteries where there is most room for improvement. Therefore, many new lithium salts has been proposed and tested.[1−14] Recently, a family of new halogen free orthoborate-based salt anions has been proposed.[12a,b,15] The unique physicochemical properties of these salts show particular promise for replacing the lithium salts used at present. The bis(oxalato)-borate (BOB^-) $[B(C_2O_4)_2]^-$ anion was found to be the most weakly associating electrolyte anion within the orthoborate-based salt family.[16] Due to its low cost, low toxicity, stability, and ease of preparation, LiBOB is currently being evaluated as a promising salt for use in lithium ion battery chemistry.[17] The exceptional performance of LiBOB in carbonate solutions in commercial type rechargeable Li ion cells is highly interesting.[18]

However, as LiBOB is a rather new material for Li ion battery chemistry, many physicochemical properties of LiBOB have not been investigated in detail. Therefore, this investigation seeks to accumulate knowledge about the fundamental properties of LiBOB, with this specific work being aimed at spectroscopic studies of the interactions between the lithium cations and the BOB anion in different solvents. For an unambiguous interpretation of the observed vibrational spectra ab initio DFT calculations on the "free" BOB anion and possible $Li^+\cdots BOB^-$ ion pairs were performed.

2. Experimental and Computational Details

The LiBOB salt was synthesized through an aqueous approach as described previously.[12a] Repeated recrystallization in appropriate solvents yields this salt of high purity (>99% by $^{11}B-NMR$ and >99.5% by Li content determination with atomic absorption spectroscopy).[19] The pure LiBOB salt was used to prepare salt solutions in different solvents with a concentration of 1 M (for some solvents concentrations of 0.5 and 2 M were used to study the concentration dependence of new vibrational modes). Dimethyl sulfoxide (DMSO), poly(ethylene glycol) (PEG, $M_w = 400$), poly(propylene glycol) (PPG, $M_w = 4000$), and deuterated PPG (d-PPG, $M_w = 2000$) were used as solvents. All solutions were prepared in a drybox (Ar) by dissolving the lithium salt in the corresponding solvents directly.

Fourier transform infrared (FT-IR) spectra were measured using a Bruker Vector 22 FT-IR spectrometer. A "golden-gate" ATR unit (Graseby Specac) was used for measuring the FT-IR spectrum of the LiBOB salt. FT-Raman spectra of the LiBOB salt and the solutions were measured using a Bruker IFS 66 interferometer equipped with a Ge-detector and coupled to a Bruker FRA 106 Raman module. A near-IR Nd:YAG laser with wavelength of 1064 nm was used as excitation source. All measurements were performed at room temperature in back-scattering geometry. The spectral resolution was $\sim 2\ cm^{-1}$ for both IR and Raman measurements.

The computational part of the studies consisted of first-principle calculations of minimum energy geometry, symmetry, and vibrational properties of "free" BOB^- and different $Li^+\cdots BOB^-$ models (**A**, **B**, and **C**) (Figure 1). All calculations were performed by using the Gaussian 03 quantum-chemical package.[20] Initially, the BOB^- anion and $Li^+\cdots BOB^-$ models were geometry optimized using symmetries (D_{2d}, C_{2v}, C_s, and C_2, respectively) by the HF/6-311+G* method.[21] Subsequent calculations of geometry and vibrational spectra were performed

* Corresponding author. E-mail: patrikj@fy.chalmers.se.
† Department of Applied Physics, Chalmers University of Technology.
‡ Department of Chemistry and Biochemistry, Arizona State University.
§ On leave from Department of Solid State Electronics, Uzhhorod National University, Uzhhorod, Ukraine.
⊥ Present address: Posnick Center of Innovative Technology, Ferro Corporation, Independence, OH 44131.

10.1021/jp0626824 CCC: $33.50
Published on Web 09/19/2006

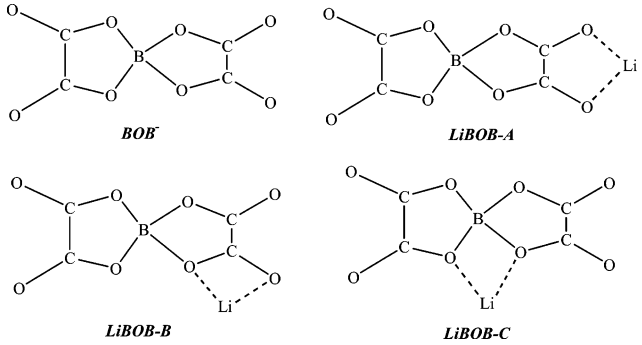

Figure 1. Structures of the BOB^- anion and the $Li^+\cdots BOB^-$ models (**A**, **B**, and **C**).

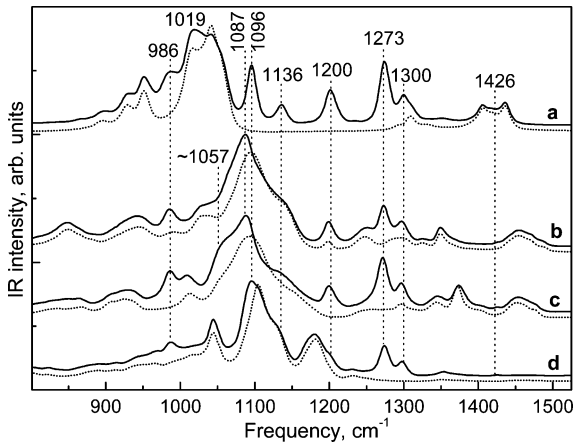

Figure 2. IR spectra of LiBOB in various solutions (solid lines) along with the spectra of the pure solvents (dotted lines): (a) DMSO (1 M); (b) PEG (1 M); (c) PPG (1 M); (d) d-PPG (0.5 M).

using the hybrid (HF+DFT) B3LYP functional consisting of a linear combination of the pure corrected exchange functional proposed by Becke[22] and the tri parameter gradient-corrected correlation functional proposed by Lee, Yang, and Parr.[23] The basis sets used for these calculations were 6-311+G* (for B and Li atoms) and Z3Pol[24] (for O and C atoms). This combination was used as the Z3Pol basis is reported to be very cost-effective to reproduce experimental IR and Raman spectra, especially with respect to IR and Raman intensities, but is unfortunately not available for B and Li atoms.[24,25] The calculated Raman and IR spectra are plotted with Lorentz functions applied (full width at half-height (FWHH) of 20 and 10 cm^{-1} were used for IR and Raman, respectively).

3. Results

3.1. IR and Raman Spectra of Solvents and LiBOB Solutions. Measured IR and Raman spectra of LiBOB solutions in different solvents together with the spectra of the corresponding solvents are shown in Figures 2 and 3, respectively. Our results show the new features in the spectra to be solvent dependent and arising either from Li^+−solvent interactions or different amounts of BOB^- anions and $Li^+\cdots BOB^-$ ion pairs present. Both these processes are detected and will be discussed in detail in the next sections. It is also possible that modes related to BOB^- or $Li^+\cdots BOB^-$ are overlapped by solvent modes and are therefore not easily resolved unless several solvents are used. Therefore, we use no less than four different solvents, with absorbance in different regions of the spectra.

3.2. Calculated Geometries and Vibrational Spectra of BOB and LiBOB Models. Our earlier calculations on BOB^- and $Li^+\cdots BOB^-$ were performed by using both HF and MP2

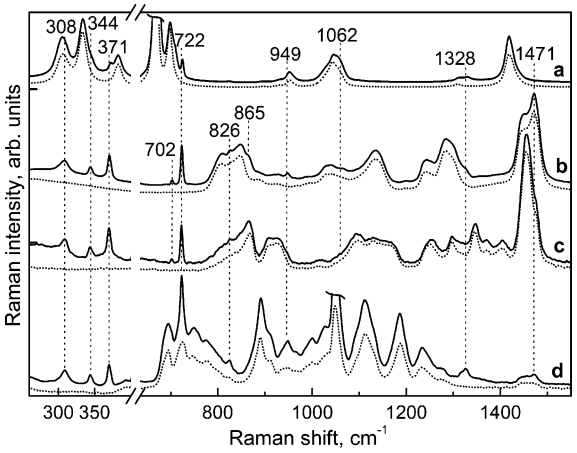

Figure 3. Raman spectra of LiBOB in various solutions (solid lines) along with the spectra of the pure solvents (dotted lines): (a) DMSO (1 M); (b) PEG (1 M); (c) PPG (1 M); (d) d-PPG (0.5 M).

methods.[26] However, ab initio DFT methods in general provide better frequencies than HF directly and use less CPU time compared with MP2 methods. Therefore, to allow for a detailed analysis of the experimental spectra DFT calculations were performed. The geometry and bonding of the model structures used for the calculations are shown in Figure 1. Symmetries, energies, and optimal geometry parameters (bond lengths and bond angles) are tabulated in Table 1. The geometry is in accordance with results from X-ray diffraction on LiBOB powder.[27] The calculated Raman and IR spectra of the BOB^- anion and the $Li^+\cdots BOB^-$ −**A** model are shown in Figure 4.

4. Discussion

4.1. Assignment of BOB and LiBOB Modes. To find unique features that in principle can be observed in experiments it is sometimes very useful to analyze the vibration properties of a system theoretically. From the literature, the assignment of the oxalate anion $[C_2O_4]^{2-}$ in the solid state and in aqueous solution is still a subject of controversy.[28,29] The frequencies of the oxalate vibrations seem to strongly depend on the internal dihedral angles.[30] Uncoordinated (aqueous) oxalate will be of point group D_{2d}[31,32] and the vibrational activity given by $\Gamma = 3A_1 + B_1 + 2B_2 + 3E$, where all modes are Raman active and the $2B_2 + 3E$ modes are also IR active. Spectra of aqueous oxalate consistent with a staggered D_{2d} configuration has been reported with fundamentals at 1486 (A_1), 1579 (B_2), 1310 (E), 900 (A_1), 761 (E), 524 (B_2) 449 (A_1), and 301 (E) cm^{-1}.[31] Upon coordination to create mono-charged oxalato species the symmetry is reduced to C_{2v}, resulting in $\Gamma = 6A_1 + 2A_2 + 5B_1 + 2B_2$[33,34] and all modes both IR and Raman active.

For the free bis(oxalato)borate anion the largest Abelian subgroup C_{2v} within the D_{2d} framework group was found computationally. The representation of the 33 modes of BOB^- is $6A_1 + 2A_2 + 3B_1 + 6B_2 + 16E$. The 16E modes are degenerate and represent only 8 unique frequencies, thus giving in total 25 unique frequencies. A mode assignment was performed for a detailed explanation of the nature of vibrational features observed in experiments (Table 2). Using the calculations 10 Raman and 7 IR active modes are identified as due to the presence of "free" BOB− anions in the solutions (Table 2 and Figure 3). Some modes cannot be detected in all the experimental spectra due to overlaps and/or low intensity.

In addition to the "free" BOB^- modes, and peaks due to the solvent used, modes were found in the IR spectra at 1019, 1087, 1136, 1300, and 1426 cm^{-1} and at 826 and ∼1062 cm^{-1} (sh)

TABLE 1: Optimal Geometry and Energies of the BOB^- Anion and $Li^+\cdots BOB^-$ Models: Distances (R, Å); Angles (∠, deg); Total Energies (E_{tot}, au) (B3LYP/6-311+G*&Z3Pol)

parameter	BOB^- (D_{2d})	LiBOB−A (C_{2v})	LiBOB−B (C_s)	LiBOB−C (C_2)	expt[a]
$R_{(B-O)1}$	1.48	1.44	1.45	1.45	1.474
$R_{(B-O)2}$		1.54	1.47	1.52	
$R_{(B-O)3}$			1.57		
$R_{(C-O)1}$	1.35	1.37	1.37	1.36	1.326
$R_{(C-O)2}$		1.30	1.30	1.39	
$R_{(C=O)1}$	1.23	1.25	1.22	1.22	1.198
$R_{(C=O)2}$		1.22	1.25	1.21	
$R_{(C-C)1}$	1.54	1.54	1.54	1.54	1.538
$R_{(C-C)2}$		1.53	1.53		
$R_{(Li-O)}$		1.89	1.93	1.89	
$\angle_{(O-B-O)1}$	105.22	108.99	108.14	105.02	109.5
$\angle_{(O-B-O)2}$	111.64	111.37	114.40	115.37	
$\angle_{(O-B-O)3}$		102.29	108.98	113.66	
$\angle_{(O-B-O)4}$			101.60	102.13	
$\angle_{(C-O-B)1}$	109.98	108.63	108.99	111.58	
$\angle_{(C-O-B)2}$		109.43	113.86	108.80	
$\angle_{(C-O-B)3}$			108.81		
$\angle_{(O=C-O)1}$	126.24	125.78	125.86	126.82	127.4
$\angle_{(O=C-O)2}$		129.98	128.61	124.27	
$\angle_{(O=C-O)3}$			119.75		
$\angle_{(O-C-C)1}$	107.41	106.87	106.94	107.57	108.0
$\angle_{(O-C-C)2}$		109.43	106.39	106.71	
$\angle_{(O-C-C)3}$			109.34		
$\angle_{(O=C-C)1}$	126.35	127.35	127.19	125.59	124.5
$\angle_{(O=C-C)2}$		120.59	125.00	128.91	
$\angle_{(O=C-C)3}$			130.91		
$\angle_{(C-O-Li)}$			83.35	123.22	
$\angle_{(C=O-Li)}$		101.62	86.00		
$\angle_{(B-O-Li)}$			167.84	90.37	
$\angle_{(O-Li-O)}$		95.58	70.89	77.12	
E_{tot}	−779.487112	−786.974629	−786.951428	−786.951045	
ΔE_{bind}[26] [kJ mol^{-1}]		558	496	508	

[a] Average distances and angles for the BOB^- ion obtained from LiBOB powder.[27]

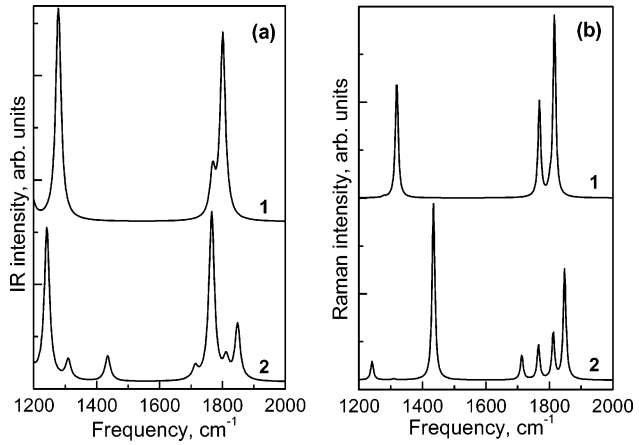

Figure 4. Calculated IR (a) and Raman (b) spectra of the BOB^- anion (1) and the $Li^+\cdots BOB^-$ −**A** model (2).

in the Raman spectra. The positions of these modes are very close to those observed in the vibrational spectra of polycrystalline LiBOB (Figure 5). To unambiguously establish the origin of these a detailed analysis of the vibrational spectra of single-crystal LiBOB is required.

The coordination of BOB^- with the lithium cation leads to decreased symmetry. In this situation all degeneracies are removed and thus additional IR and/or Raman modes might become visible. The realization of one (or more) $Li^+\cdots BOB^-$ models (Figure 1) in the solutions (i.e., the existence of $Li^+\cdots BOB^-$ ion pairs) would influence the vibrational spectra. However, it is unfortunately not possible to identify the $Li^+\cdots BOB^-$ ion pairs directly by their Li−O stretching vibrations, due to the very low intensities of these modes. The main features expected, from the ion pairing effect, are shifts or splits of the modes corresponding to the BOB^- C═O vibrations (∼1800−1820 cm^{-1}) in both the IR and Raman spectra. However, according to the calculations the best feature to use to identify structure **A** is the Raman active mode at 1435 cm^{-1}. This mode corresponds to C−C stretching and becomes a strong Raman active mode in structure **A**. The structure **A** ion pair is the most likely ion pair based on the binding energies (Table 1,[26]), and we therefore initially focus on this ion pair.

4.2. Li^+ Coordination. As mentioned, at least two effects related to the coordination of the lithium cation can be observed in the spectra, below these are discussed separately starting with the cation−solvent interaction. To assist in the interpretation, the experimental spectra of LiBOB solutions were compared both with calculated spectra and with the spectrum of polycrystalline LiBOB.

4.2.1. Li^+ Coordination with Solvent(s). A Raman active mode at ∼865 cm^{-1} was observed in the Raman spectra of LiBOB in PEG (Figure 6). Also, the Raman intensity of this mode is growing with the concentration of LiBOB. The IR intensity of this mode was found to be very low. As any 865 cm^{-1} band was not found in the calculated spectra of either LiBOB models nor in polycrystalline LiBOB the nature of this mode cannot be explained by $Li^+\cdots BOB^-$ interactions.

On the other hand, a strong Raman active band has been observed in the frequency range 860−870 cm^{-1} for many PEO-MX complexes (PEO = poly(ethylene oxide), M = alkali cation, X = monovalent anion), while it is absent in uncomplexed PEO.[35,36] The corresponding calculated modes for the lithium ion−tetraglyme complexes, and indeed also for the penta- and hexaglyme complexes, reveal that regardless of chain conformation a similar Raman active band exists.[37] It is assigned to a symmetric A_{1g} mode involving a metal−oxygen ring breathing

TABLE 2: Selected Vibration Mode Frequencies (ω, cm^{-1}), IR (I_{calc}^{IR}, km/mol) and Raman (I_{calc}^{Raman}, Å^4/amu) Intensities of (A) BOB^- and (B) $Li^+\cdots BOB-A$, $-B$, and $-C$ Pairs (B3LYP/6-311+G*&Z3Pol, with the Estimated Error in the Computed Frequencies based on BOB^- ($\Delta\omega$) < 8 cm^{-1})[a]

(a)

ω BOB^-	I_{calcd}^{IR}	I_{calcd}^{Raman}	ω $C_2O_4^{2-}$ [b]	IR^{expt} [c]	Raman^{expt} [c]	tentative assignment
71 (E)	3.6	1.2				torsional vibrations
82 (B_1)	−	2.3				
144 (A_2)	−	−				
299 (A_1)	−	3.8				
			301 (E)			
311 (B_1)	−	0.2			308	t(B−O_2 groups of BO_4)
339 (B_2)	9.2	1.3			344	b(O═C−C═O)
362 (E)	0.1	0.2				b(B−O−C═O) + t(C_2O_4, ring)
365 (A_1)	−	4.4			371	b(O═C−C═O) + breathing mode
			449 (A_1)			
489 (E)	29.1	−				δ(O═C−O)
			524 (B_2)			
598 (E)	4.6	2.5				δ(O−C−C)
672 (E)	−	−				δ(O−B−O) + δ(O═C−O)
707 (B_2)	9.0	1.6		703	702	δ(O−B−O)
724 (A_1)	−	13.4			722	δ(O−B−O) + rings breathing
			761 (E)			
844 (A_2)	−	−				δ(O−C═O) + b(C−C)
844 (B_1)	−	0.2				δ(O−C═O) + b(C−C)
853 (B_2)	1.0	0.4				δ(O−C═O) + δ(rings)
			900 (A_1)			
942 (A_1)	−	8.0			949	$\nu_{full\ s}$(O−B−O) + δ(O−C−O)
995 (E)	153.3	−		986		ν_{as}(O−B−O)
1119 (B_2)	1145.3	1.0		1096		ν_s(O−B−O)
1187 (E)	134.5	−		1200		$\nu_{n\varphi}$(C−O)
1278 (B_2)	1279.6	0.5		1273		$\nu_{n\varphi}$(C−O) + ν(C−C)
			1310 (E)			
1320 (A_1)	−	52.2			1328	ν_φ(C−O) + ν(C−C)
			1486 (A_1)			
			1579 (B_2)			
1769 (E)	133.8	20.9		1780	1780	$\nu_{n\varphi}$(C═O)
1801 (B_2)	1118.7	3.9		1804	1804 (sh)	$\nu_{n\varphi}$(C═O)
1816 (A_1)	−	80.8			1822	ν_φ(C═O)

(b)

ω LiBOB−A	I_{calcd}^{IR}	I_{calcd}^{Raman}	ω LiBOB−B	I_{calcd}^{IR}	I_{calcd}^{Raman}	ω LiBOB−C	I_{calcd}^{IR}	I_{calcd}^{Raman}
400 (A_1)	w	vw	352 (A′)	w	vw	309 (B)	w	vw
448 (B_2)[d]	vw	vw	383 (A′)[d]	w	vw	390 (B)[d]	vw	vw
478 (B_2)	w	vw	476 (A′)	w	vw	477 (B)	w	0
479 (B_1)	w	vw	495 (A″)	w	0	508 (A)[d]	m	vw
529 (A_1)[d]	m	vw	507 (A′)[d]	m	vw	721 (A)	w	w
608 (B_2)	w	vw	584 (A′)	w	vw	826 (B)	m	vw
687 (A_1)	w	vw	660 (A′)	w	vw	905 (A)	w	w
734 (A_1)	vw	w	710 (A′)	w	vw	918 (B)	s	vw
890 (B_2)	m	vw	731 (A′)	vw	w	996 (A)	w	vw
937 (A_1)	vw	m	847 (A′)	w	vw	1090 (B)	m	vw
1027 (B_1)	w	0	897 (A′)	m	w	1147 (A)	m	vw
1118 (A_1)	vs	w	962 (A′)	w	w	1172 (B)	s	vw
1181 (B_1)	m	0	1025 (A″)	w	0	1225 (B)	vs	vw
1242 (A_1)	s	w	1151 (A′)	s	w	1267 (A)	0	s
1310 (B_2)	m	vw	1170 (A″)	m	0	1810 (B)	m	s
1435 (A_1)	m	vs	1195 (A′)	m	vw	1812 (A)	m	m
1713 (B_2)	m	m	1246 (A′)	vs	w	1839 (B)	s	w
1766 (A_1)	vs	m	1331 (A′)	m	s	1850 (A)	vw	vs
1812 (B_1)	m	s	1716 (A′)	m	s			
1848 (A_1)	s	s	1808 (A″)	m	s			
			1817 (A′)	s	s			
			1844 (A′)	m	vs			

[a] Descriptions: I_{calcd}^{IR} = vs (>1000), 300 < s < 1000, 50 < m < 300, 15 < w < 50, vw (<15); I_{calcd}^{Raman} = vs (>50), 20 < s <50, 10 < m <20, 5 < w < 10, vw(<5); t, b, δ, ν_s, ν_{as}, ν_φ and $\nu_{n\varphi}$ = torsional, bending, deformational, and valence (symmetric, asymmetric, in-phase and out-of-phase) vibrations, respectively. [b] Experimental fundamental modes of aqueous oxalate with a staggered D_{2d} symmetry.[31] [c] Modes characteristic for BOB^- observed in the solution spectra. [d] Symmetric and asymmetric Li−O stretching modes.

motion.[36] The fact that this mode characteristic of the complexes is not observed in IR spectra may indicate a (quasi)-symmetric ordering of oxygen atoms around the lithium cation. Thus, even PEG, a low dielectric constant solvent, coordinates the cation quite strongly, supporting the LiBOB salt as very dissociative.[12,16,26] The cation coordination by the solvent is not explicitly observed or discussed here for the other solvents used (DMSO, PPG, or d-PPG), but is highly likely for a strong dielectric solvent like DMSO, while considerably less likely for PPG − due to the steric hindrance that the extra methyl

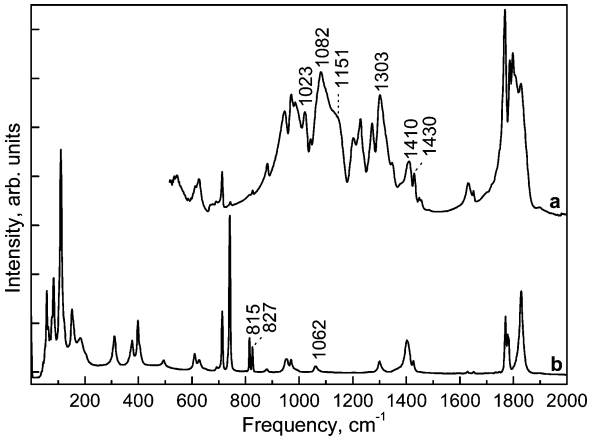

Figure 5. IR (a) and Raman (b) spectra of polycrystalline LiBOB.

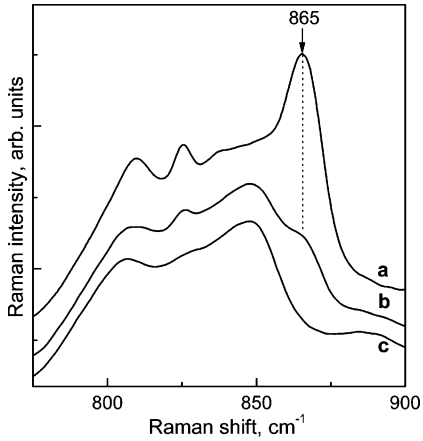

Figure 6. Concentration dependent Raman spectra of LiBOB in PEG: (a) 2 M; (b) 1 M; (c) pure PEG.

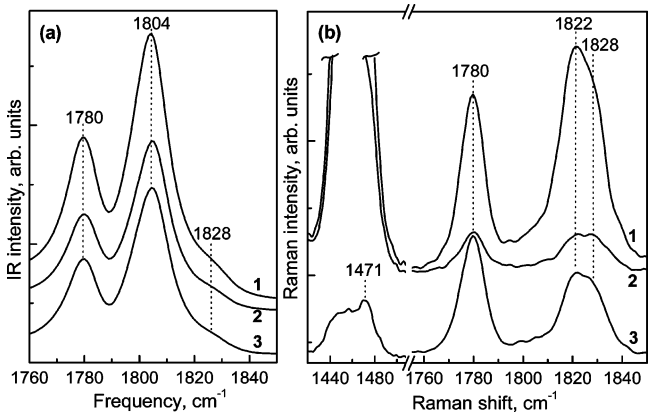

Figure 7. Selected regions of IR (a) and Raman (b) spectra of LiBOB in PPG (curve 1, 1.0 M; curve 2, 0.5 M) and d-PPG (curve 3, 0.5 M).

group compared with PEG should bring about. These are is also the reasons why we primarily expect to find signs of ion pairs of $Li^+\cdots BOB^-$ in the PPG solutions, if anywhere. Still, however, the cation−solvent interaction should be dominant.

4.2.2. Li^+ Coordination with Anion(s). While peaks that can be directly related with the $Li^+\cdots BOB^-$ models were not observed in either IR nor Raman spectra of LiBOB in any of the solvents, a broadening of the C═O band vibrations was found both in the IR and the Raman spectra of LiBOB in PPG (Figure 7). As this feature was promising as a signature of $Li^+\cdots BOB^-$ ion pairing it was studied in detail. First, a lower salt concentration was used (0.5 M) to ensure this feature to be concentration dependent. As can be seen in Figure 7 the new mode at ∼1828 cm^{-1} exists in all the vibrational spectra. In addition, the mode is considerably more intense in Raman and according to the calculations the feature at 1828 cm^{-1} can be related with either one of the ion pair models: **A**, **B**, or **C** (Table 2). The reason for the apparently very small intensity of the 1828 cm^{-1} band in IR is that the "free" BOB^- feature at 1804 cm^{-1} is so very dominant in the IR spectra.

Using the FT-IR spectra of LiBOB (1 M) in different solvents, the calculated ratio (I_{1780}/I_{1804}) was found to be ∼0.6 for all 1 M LiBOB solutions (DMSO, PEG, and PPG). This ratio can in general be useful for identification of both the amount and type of Li BOB^- pair realized. According to the calculated IR spectra of the ion pair models only structure **A** has a strong IR active mode (calculated 1766 cm^{-1}) that can contribute to the 1780 cm^{-1} peak (Figure 4a). However, only a very small increase of I_{1780}/I_{1804} (0.58 to 0.61; ∼5%) was found upon increasing the concentration of LiBOB in PPG from 0.5 to 1 M.

As discussed earlier, structure **A** has a unique feature in Raman calculated at 1435 cm^{-1}. Neither "free" BOB^- nor the **B** or **C** ion pairs have any bands in this region. Yet, this peak cannot be resolved experimentally in the PPG solutions as the CH_2 groups of PPG have vibrations with strong Raman intensity in the same frequency range (Figure 3c). To resolve this situation these modes were shifted down below 1200 cm^{-1} by using d-PPG as solvent. A Raman mode at 1472 cm^{-1} then becomes clearly visible (Figure 3d and 7) and we assign this to structure **A** (calc. 1435 cm^{-1}). The underlying broad feature is due to incomplete deuteration (Figure 3d). As can be seen in Figure 7, parts a and b, also the features at 1828 cm^{-1} in PPG remain in d-PPG.

In principle, also the peaks observed at ∼900 cm^{-1} in IR and the broadenings of the IR peaks at ∼1100 and 1140 cm^{-1} may correspond to ion pairs (Figure 2). As these features were promising as signatures of $Li^+\cdots BOB^-$ ion pairing IR and Raman spectroscopy of these regions can be used to detect ion pairs, but any unambiguous identification of the type of $Li^+\cdots BOB^-$ ion pair (**A**, **B**, or **C**) seems difficult as all ion pairs may contribute in these regions.

4.3. Comparison with Other Lithium Salts. IR and Raman spectroscopies have both been used extensively to analyze the dissociation of various lithium salts in aprotic solvents. The $LiClO_4$ and $LiBF_4$ salts were early studied in PPO/PPG.[38−40] Only for very high salt concentrations, or elevated temperatures, the $LiClO_4$ PPO system showed signs of ion pairs, detectable as a 6−8 cm^{-1} upshifted shoulder on the strong ∼930 cm^{-1} ν_1 ClO_4^- vibration. $LiBF_4$ much more readily forms spectroscopically detectable ion pairs in PPO.[39] One of the more common anions for spectroscopic analysis of ion pairs in electrolytic solutions is $CF_3SO_3^-$ (Tf). Among the early work, Bernson and Lindgren[41] and Stevens and Jacobsson[39] used IR and Raman spectroscopy, respectively, to elucidate the formation of $Li^+\cdots Tf^-$ ion pairs in PPO. While some arguments differ on the assignments, both rather easily found $Li^+\cdots Tf^-$ ion pair formation.

More recently both the $LiPF_6$ and LiTFSI salts have been studied as solutes. PF_6^- is arguably a very weakly coordinating anion, as shown also by its use in Li-batteries, and it was only with difficulty that Aroca et al. assigned a 23 cm^{-1} shift of the 844 cm^{-1} ν_3 PF_6^- band for 1 M $LiPF_6$ in DMC to the existence of $Li^+\cdots PF_{6-}$ ion pairs.[42] Burba and Frech[43] elegantly performed an analysis based on the perturbation, caused by cation contact, to the ν_1 mode (∼741 cm^{-1}), and thereby detected an IR activity of this, if unperturbed, IR inactive mode. The presence is thus a sign of ion pairs and its size proportional to the number of ion pairs. They additionally observed the same shifts as Aroca

et al. of the ν_3 vibration. For the TFSI− anion, the choice of anion band as reference is less obvious as the anion has only C_2 symmetry. One band that has found use is the ~741 cm^{-1} band, assigned as due to the entire anion expanding and contracting.[44] Rey et al. found no signs of ion pairs in neither in IR nor in Raman spectra of $LiTFSIPEO_n$ even for $n = 8$ using this band,[44,45] but by use of very high salt concentrations (5 M) in a gel electrolyte, substantial ion association was observed.[46] In the latter work, no ion pairs were observed for 1 M systems. Later, Brouillette et al. found clear signs of $Li^+\cdots TFSI^-$ ion pairs in different PEO-oligomers for high concentrations, 10.4−2.0 mol kg^{-1} ($4 < n < 13$), by Raman spectroscopy.[47]

Thus, from spectroscopic literature there is no common investigation dealing with all these salts using the same solvent, etc. Yet, we can conclude that for the $LiBF_4$ and LiTf salts ion pairs are rather easily found, while for $LiClO_4$, $LiPF_6$, and LiTFSI they are elusive. Even if we have been unable to make very strong solutions, LiBOB should be among the latter salts, as shown by the very small ion pair related features. This overall picture is supported also by our recent computational work,[26,48] where we find the order of lithium ion−anion interaction strength to be as follows: $BF_4^- > Tf^- > TFSI^- \approx PF_6^- > BOB^-$. This is in good agreement also with our earlier study:[49] $BF_4^- > Tf^- > TFSI^- > ClO_4^- \approx PF_6^-$.

5. Conclusions

The geometrical parameters of computed "free" BOB^- are in good accordance with those obtained for LiBOB powder. By combining experimental and computed IR and Raman spectra the lithium ion coordinating properties of the new orthoborate BOB^- anion were investigated. The BOB^- anion was found to be spectroscopically "free" in DMSO and PEG solutions. In PPG a small shoulder at 1828 cm^{-1} probably corresponding to $Li^+\cdots BOB^-$ ion pairs were found in the Raman spectra. The calculations, energies, and spectra, together with the small feature at 1472 cm^{-1} in the Raman spectra of LiBOB in d-PPG, further support the **A** $Li^+\cdots BOB^-$ ion pair to be the preferred type of ion pair and present in a very small amount in 0.5 M LiBOB in d-PPG. In addition, a distinct Raman mode at 865 cm^{-1} was found in the PEG solutions, indicating strong Li^+−solvent coordination. Compared with other Li salts the LiBOB salt seems promising also with respect to the degree of dissociation.

Acknowledgment. R.H. acknowledges a scholarship from the Swedish Institute for this project at the Department of Applied Physics, Chalmers University of Technology. The authors sincerely thank Dr. Daniel Andersson, Chalmers for providing the d-PPG. Also the helpful technical assistance of Dr. Ezio Zanghellini is gratefully acknowledged. The calculations in this article have mainly been carried out at the Condensed Matter Physics Linux cluster.

Supporting Information Available: Color versions of Figures 2 and 3. This material is available free of charge via the Internet at http://pubs.acs.org.

References and Notes

(1) Johansson, P.; Jacobsson, P. *J. Power Sources* **2006**, *153*, 336.
(2) Jasinski, R.; Carroll, S. *J. Electrochem. Soc.* **1970**, *117*, 218.
(3) Ue, M. *J. Electrochem. Soc.* **1994**, *141*, 3336.
(4) Abraham, K. M.; Goldman, J. L.; Natwig, D. L. J. *J. Electrochem. Soc.* **1982**, *129*, 2404.
(5) Webber, A. J. *J. Electrochem. Soc.* **1991**, *138*, 2586.
(6) Dominey, L. A.; Koch, V. R.; Blakely, T. *Electrochim. Acta* **1992**, *37*, 1551.
(7) Krause, L. J.; Lamanna, W.; Summerfield, J.; Engle, M.; Korba, G.; Loch, R.; Atanasoski, R. *J. Power Sources* **1997**, *68*, 320.
(8) Barthel, J.; Buestrich, R.; Gores, H. J.; Schmidt, M.; Wühr, M. *J. Electrochem. Soc.* **1997**, *144*, 3866.
(9) Handa, M.; Suzuki, M.; Suzuki, J.; Kanematsu, H.; Sasaki, Y. *Electrochem. Solid-State Lett.* **1999**, *2*, 60.
(10) Gnanaraj, J. S.; Zinigrad, E.; Levi, M. D.; Aurbach, D.; Schmidt, M. *J. Power Sources* **2003**, *119/121*, 799.
(11) Egashira, M.; Scrosati, B.; Armand, M.; Béranger, S.; Michot, C. *Electrochem. Solid-State Lett.* **2003**, *6*, A71.
(12) (a) Lischka, U.; Wietelmann, U.; Wegner, M. Ger. DE 19829030 C1 1999; (b) Xu, W.; Angell, C. A. *Electrochem. Solid-State Lett.* **2001**, *4*, E1.
(13) Xu, W.; Angell, C. A. *Electrochem. Solid-State Lett.* **2000**, *3*, 366.
(14) Yamaguchi, H.; Takahashi, H.; Kato, M.; Arai, J. *J. Electrochem. Soc.* **2003**, *150*, A312.
(15) Videa, M.; Xu, W.; Geil, B.; Marzke, R.; Angell, C. A. *J. Electrochem. Soc.* **2001**, *148*, A1352.
(16) Xu, W.; Shusterman, A. J.; Videa, M.; Velikov, V.; Marzke, R.; Angell, C. A. *J. Electrochem. Soc.* **2003**, *150*, E74.
(17) Xu, K.; Zhang, S. S.; Lee, U.; Allen, J. L.; Jow, T. R. *J. Power Sources* **2005**, *146*, 79.
(18) Xu, K.; Zhang, S. S.; Jow, T. R.; Xu, W.; Angell, C. A. *Electrochem. Solid-State Lett.* **2002**, *5*, A26.
(19) Xu, K.; Zhang, S.; Poese, B. A.; Jow, T. R. *Electrochem. Solid-State Lett.* **2002**, *5*, A259.
(20) Frisch, M. J.; Trucks, G. W.; Schlegel, H. B.; Scuseria, G. E.; Robb, M. A.; et al. Gaussian, Inc.: Pittsburgh, PA, 2003.
(21) Rassolov, V. A.; Pople, J. A.; Ratner, M. A.; Windus, T. L. *J. Chem. Phys.* **1998**, *109*, 1223.
(22) Becke, A. D. *Phys. Rev. A* **1998**, *38*, 3098.
(23) Lee, C.; Yang, W.; Parr, R. G. *Phys. Rev. B* **1998**, *37*, 785.
(24) Benkova, Z.; Sadlej, A. J.; Oakes, R. E.; Bell, S. E. J. *J. Comput. Chem.* **2005**, *26*, 145.
(25) Oakes, R. E.; Bell, S. E. J.; Benkova, Z.; Sadlej, A. J. *J. Comput. Chem.* **2005**, *26*, 154.
(26) Markusson, H.; Johansson, P.; Jacobsson, P. *Electrochem. Solid-State Lett.* **2005**, *8*, A215.
(27) Zavalij, P. Y.; Yang, S.; Whittingham, M. S. *Acta Crystallogr.* **2003**, *B59*, 753.
(28) Shippey, T. A. *J. Mol. Struct.* **1980**, *67*, 223.
(29) Hind, A. R.; Bhargava, S. K.; Van Bronswijk, W.; Grocott, S. C.; Eyer, S. L. *Appl. Spectrosc.* **1998**, *52*, 683.
(30) Dinnebier, R. E.; Vensky, S.; Panthöfer, M.; Jansen, M. *Inorg. Chem.* **2003**, *42*, 1499.
(31) Begun, G. M.; Fletcher, W. H. *Spectrochim. Acta* **1963**, *19*, 1343.
(32) Chumaevskii, N. A.; Sharopov, O. U.; Minaeva, N. A. *Zh. Neorg. Khim.* **1988**, *33*, 1390.
(33) Edwards, H. G. M.; Farwell, D. W.; Rose, S. J.; Smith, D. N. *J. Mol. Struct.* **1991**, *249*, 233.
(34) Edwards, H. G. M.; Hardman, P. H. *J. Mol. Struct.* **1992**, *273*, 73.
(35) Brodin, A.; Mattsson, B.; Nilsson, K.; Torell, L. M.; Hamara, J. *Solid State Ionics* **1996**, *85*, 111.
(36) Torell, L. M.; Schantz, S. *Polymer Electrolyte Reviews 2*; MacCallum, J. R., Vincent, C. A., Eds.; Elsevier Applied Science: London, 1989; p 1.
(37) Johansson, P.; Tegenfeldt, J.; Lindgren, J. *Polymer* **1999**, *40*, 4399.
(38) Schantz, S.; Torell, L. M.; Stevens, J. R. *J. Appl. Phys.* **1988**, *64*, 2038.
(39) Stevens, J. R.; Jacobsson, P. *Can. J. Chem.* **1991**, *69*, 1980.
(40) Frech, R.; Manning, J. P. *Electrochim. Acta* **1992**, *37*, 1499.
(41) Bernson, A.; Lindgren, J. *Solid State Ionics* **1993**, *60*, 37.
(42) Aroca, R.; Nazri, M.; Nazri, G. A.; Camargo, A. J.; Trsic, M. *J. Solution Chem.* **2000**, *29*, 1047.
(43) Burba, C. M.; Frech, R. *J. Phys. Chem. B* **2005**, *109*, 15161.
(44) Rey, I.; Johansson, P.; Lindgren, J.; Lassègues, J. C.; Grondin, J.; Servant, L. *J. Phys. Chem. A* **1998**, *102*, 3249.
(45) Rey, I.; Lassègues, J. C.; Grondin, J.; Servant, L. *Electrochim. Acta* **1998**, *43*, 1505.
(46) Abbrent, S.; Lindgren, J.; Tegenfeldt, J.; Wendsjö, Å. *Electrochim. Acta* **1998**, *43*, 1185.
(47) Brouillette, D.; Irish, D. E.; Taylor, N. J.; Perron, G.; Odziemkowski, M.; Desnoyers, J. E. *Phys. Chem. Chem. Phys.* **2002**, *4*, 6063.
(48) Johansson, P.; Jacobsson, P. *Solid State Ionics*, in press.
(49) Johansson, P.; Jacobsson, P. *J. Phys. Chem. A* **2001**, *105*, 8504.